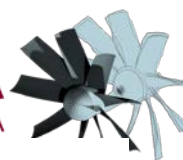


***NUMERICAL STRATEGIES FOR INVESTIGATION OF AN
AXIAL FLOW FAN WITH AN ANTI-STALL RING IN TUNNEL
AND METRO APPLICATIONS***

A. Corsini - G. Delibra - D. Volponi



SAPIENZA
UNIVERSITÀ DI ROMA
TITM @ DIMA-URLS



www.dima.uniroma1.it

Fans: are everywhere and have a very complex market:

- Small and specialised enterprises
- Large corporations producing all kind of fans (from laptop to wind tunnel)

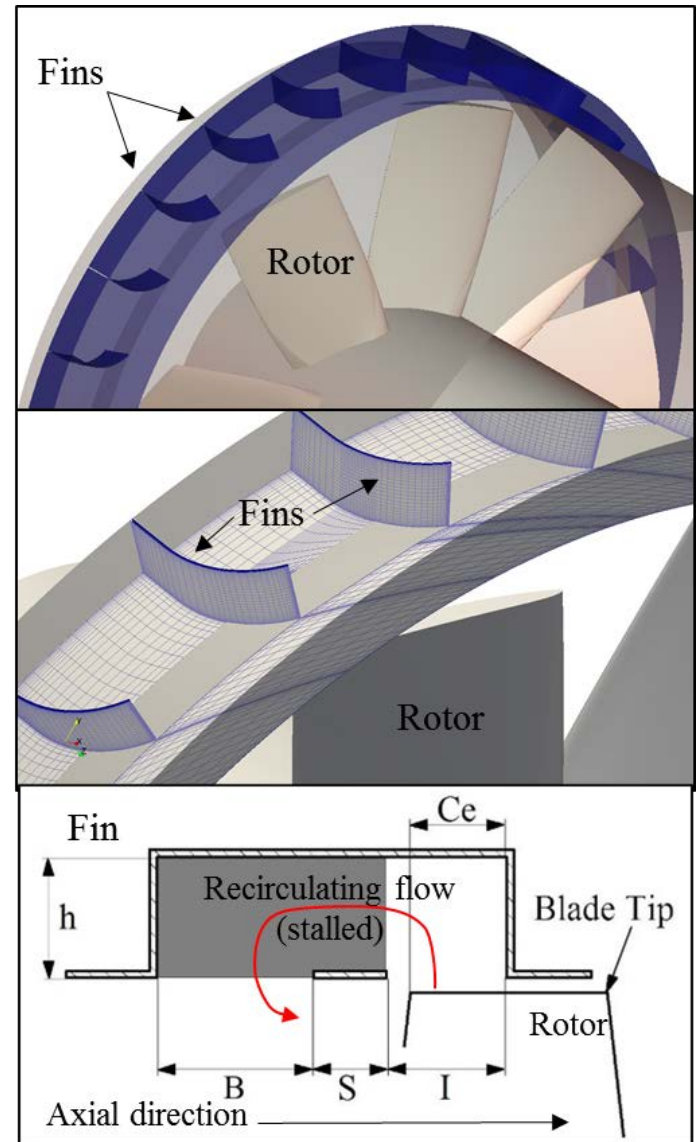
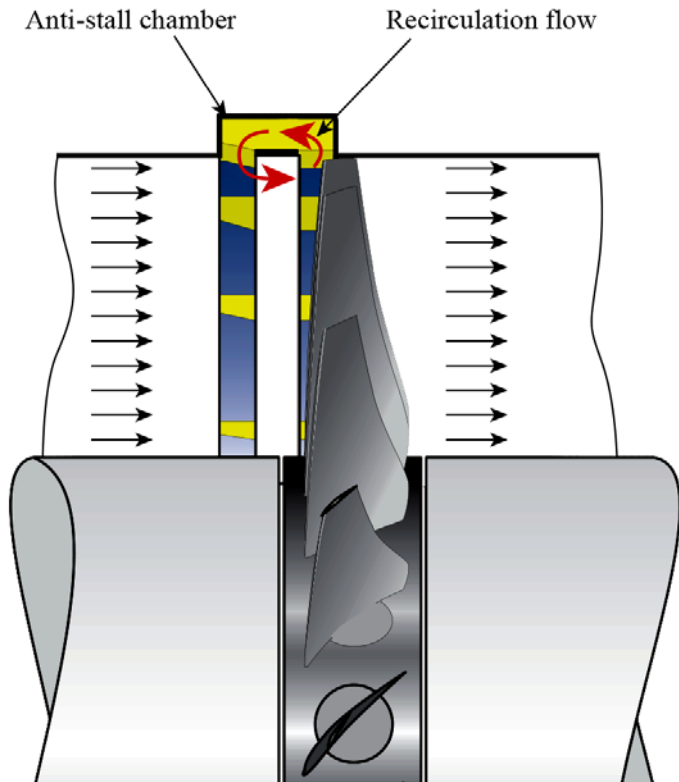
... now driven by legal requirements on minimum efficiency grades within EU and USA, and soon worldwide

- For Europe: EU Commission Regulation No. 327/2011, mandating minimum Fan and Motor Efficiency Grades (FMEG's)
Commission Regulation (EU) No. 327/2011, Official Journal of the European Union, 1st June 2011

... and many more kind of legal requirements on noise, safety and so on

Here we are referring to tunnel and metro fan market for ventilation and focus on stall control technologies, in particular to a so-called antistall ring

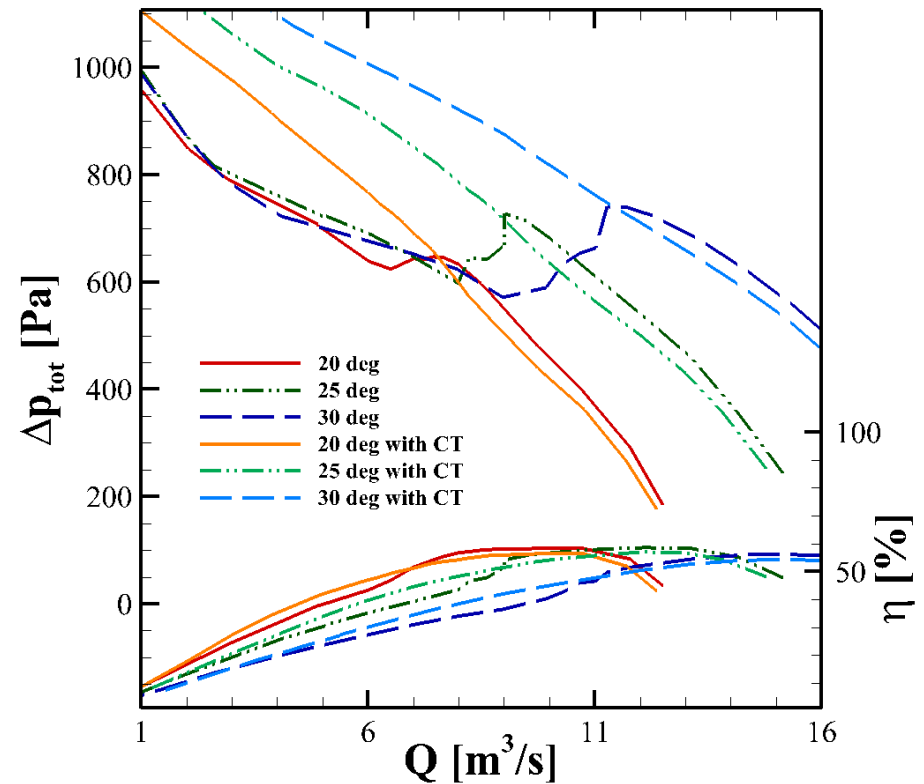
A antistall ring consists of an annular chamber which is incorporated in the fan casing, fitting over the fan blades' leading edge. The vanes are classically constructed from curved plate, welded into the annular chamber with a shroud to separate stabilisation ring inlet and discharge.



In experiments the stabilisation ring's impact is apparent. At peak pressure the stabilisation ring has almost no impact on either fan pressure rise or efficiency.

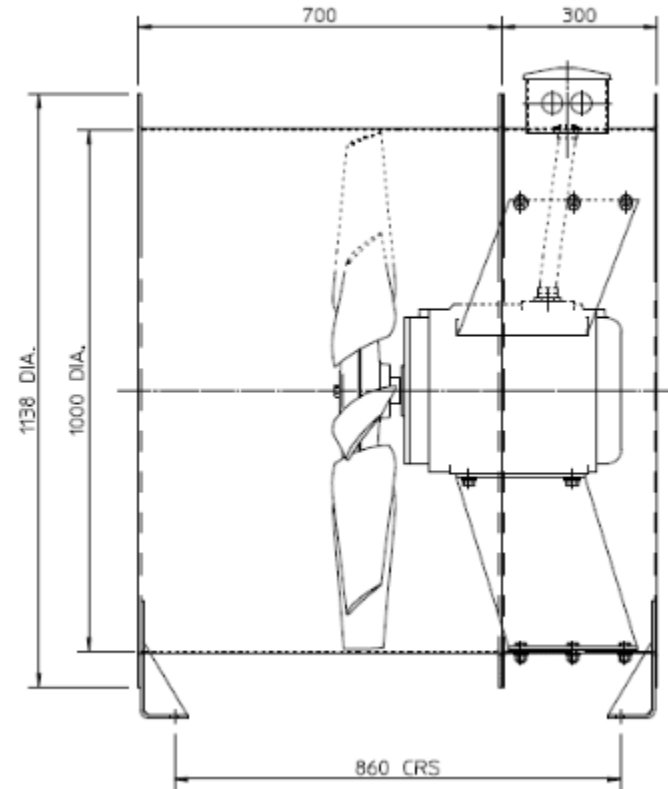
As flow reduces and the fan stalls, the stabilisation ring's effect is to eliminate the drop in pressure, with continuously rising pressure back to zero flow.

The stabilisation ring increases both the fan's pressure developing capability and efficiency at lower flow rates that would occur with stall if there were no fitted stabilisation ring.



Sketch of the tested Fan

<i>Blade section</i>	<u>Reversible(*)</u>
<i>Diameter at the tip</i>	1000 mm
<i>Blade count</i>	9
<i>Hub-to-tip ratio</i>	0.4
<i>Rotational speed</i>	1490 rpm



(*) this actually means that aerodynamically the performance of this fan are severely compromised with respect to optimum

Here I briefly summarize different strategies adopted to numerically study the mechanism of flow control induced by the antistall ring and to actually derive an industrial way to optimize the shape of the ring and its fins.

Stall control mechanism investigation:

1. Steady state frozen rotor investigation: RANS with MRF and AMI coupling
2. Unsteady rotor stator interaction: URANS with moving mesh and AMI coupling

Antistall ring optimization

3. Novel strategy to account for the effect of the fins: RANS with MRF, AMI coupling and antistall ring modelled with an advanced actuator disk

STALL CONTROL MECHANISM

1. STEADY STATE FROZEN ROTOR INVESTIGATION: RANS WITH MRF AND AMI COUPLING

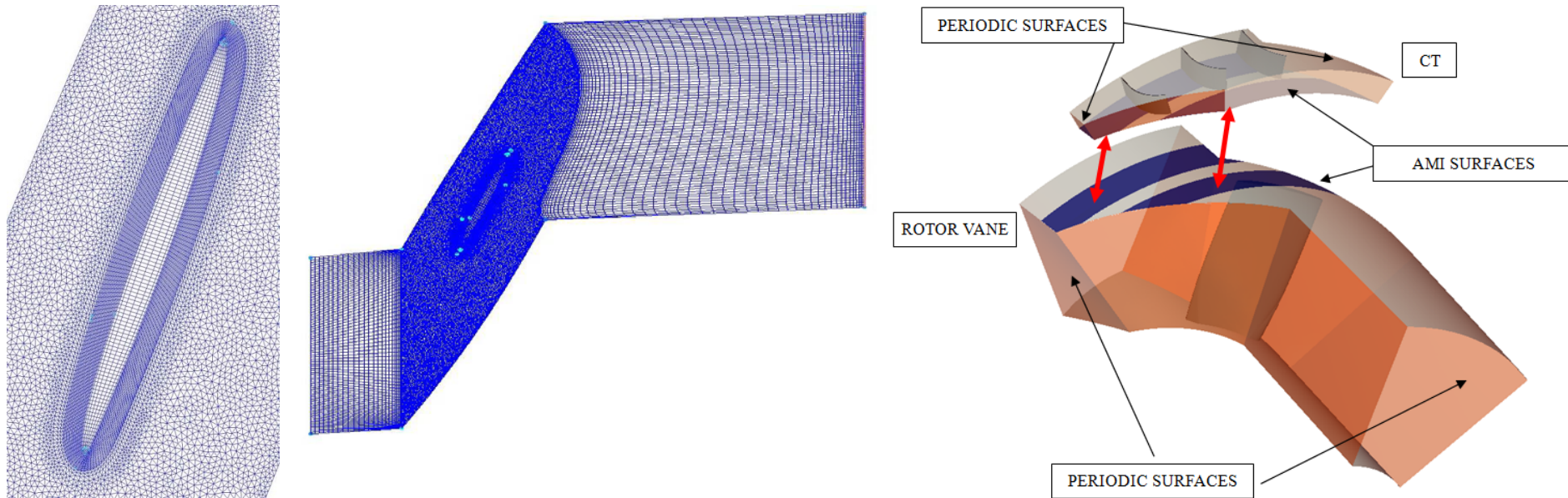


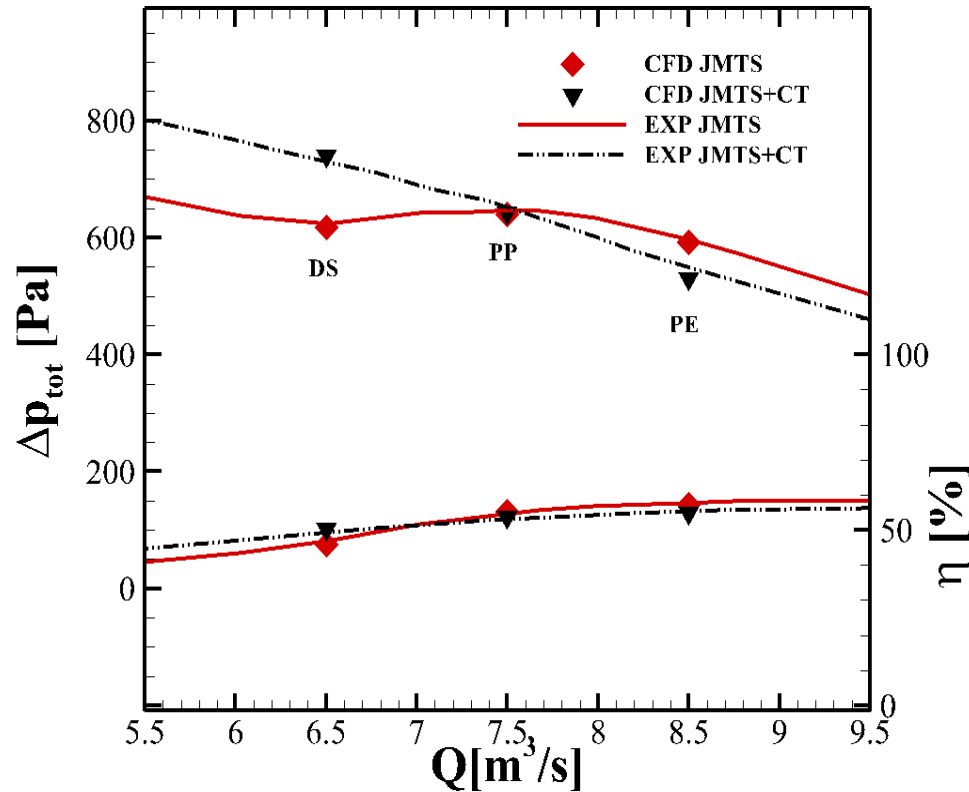
1. INVESTIGATION OF STALL CONTROL MECHANISM

Fan pressure rise, blade lift and drag were used as convergence parameters for grid sensitivity analysis with grids of 1.2, 4.0 and 7.5 million cells.

Final grid for the studied fan's computational analysis without fitted stabilisation ring comprised 2.0 million hexahedra and 4.5 million tetrahedral

The final grid for the studied fan's computational analysis with a fitted stabilisation ring included an additional 1.0 million hexahedra.





Three operating points were computed corresponding to:

Deep Stall (DS)

Peak Pressure (PP)

Maximum Efficiency (PE)

The methodology allowed to reconstruct the curves with fair agreement for all the operating points.

The slight over-prediction of efficiency can be explained with the simulation taking into account a motor efficiency of 100%.

PE

PP

DS

LE

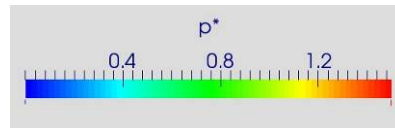
NO CT

TE

CT

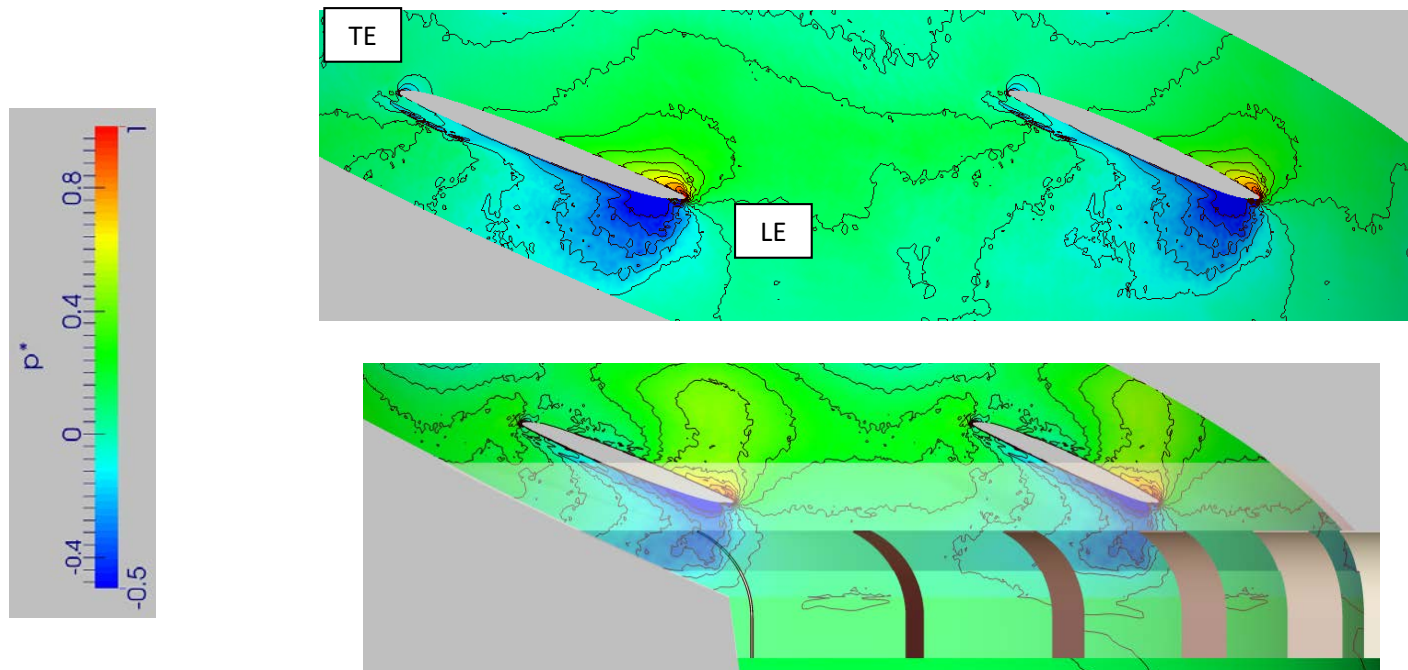
Normalised pressure contours over the blade pressure surface with and without a fitted stabilisation ring provide an insight into the span-wise flow-field.

A stabilisation ring fitted over the blade tip leading edge eliminates a separation at the blade hub trailing edge.



The absence of the hub separation indicates that the stabilisation ring has affected blade loading over the entire blade span.

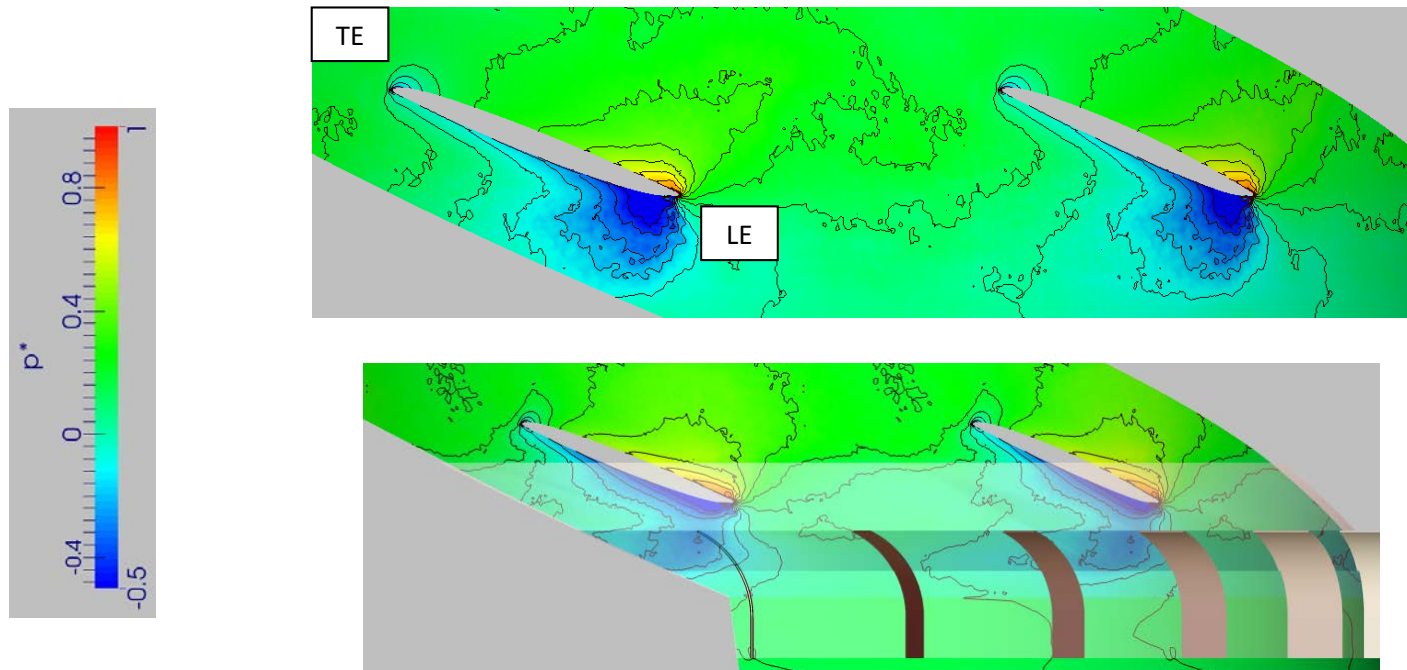
The presence of a stabilisation ring results in a small reduction in a negative pressure core's magnitude at the blade leading edge.



Peak Efficiency operating point pressure contours

Reduction could be associated with the flow that diverts into the stabilisation ring annular cavity.

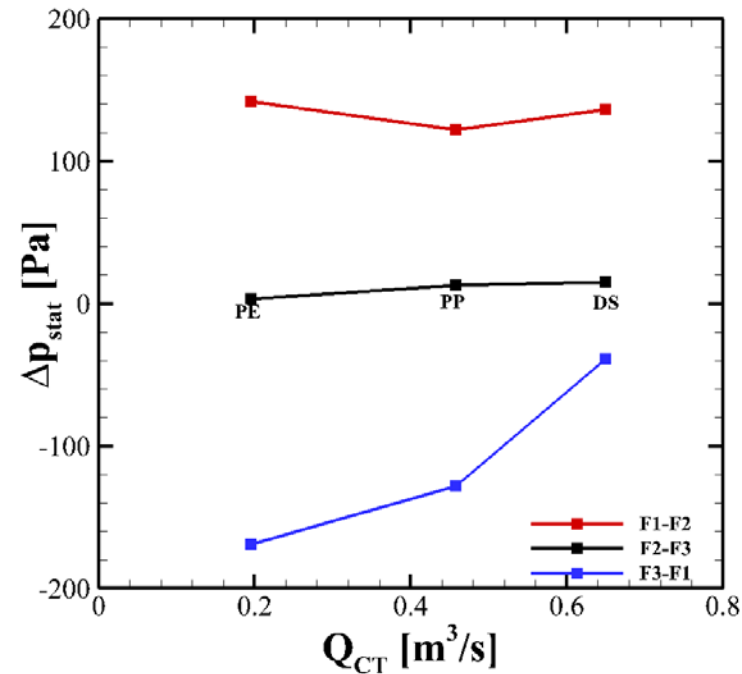
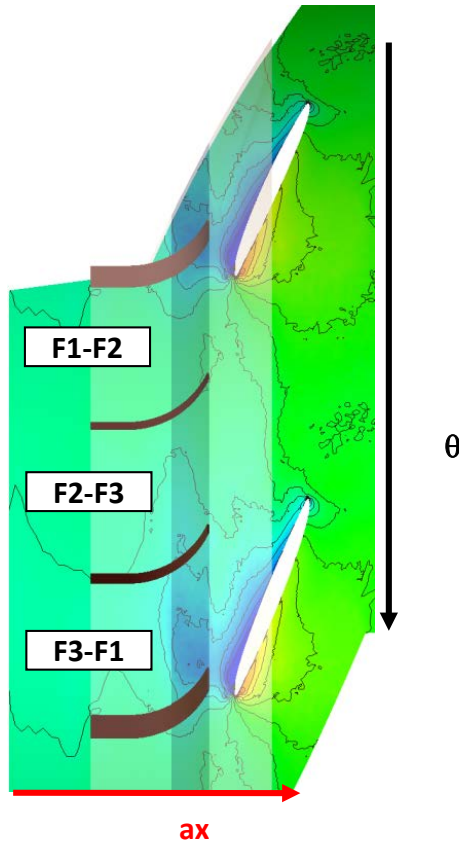
Trends that we observed with the move from the peak efficiency to the peak pressure operating point continue. Both suction surface negative pressure and pressure surface high pressure cores are clearly defined along the blade chord, indicating that the control of boundary layer fluid has now become more fully established.



Peak Pressure operating point pressure contours

The stabilisation ring's presence has resulted in a blade-to-blade flow-field that feeds boundary layer fluid into the stabilisation ring annular chamber.

To give additional hints about the azimuthal behavior of the CT let's take the static pressure difference evolution inside each CT vane against the volume flow rate, when throttling the fan to stall.

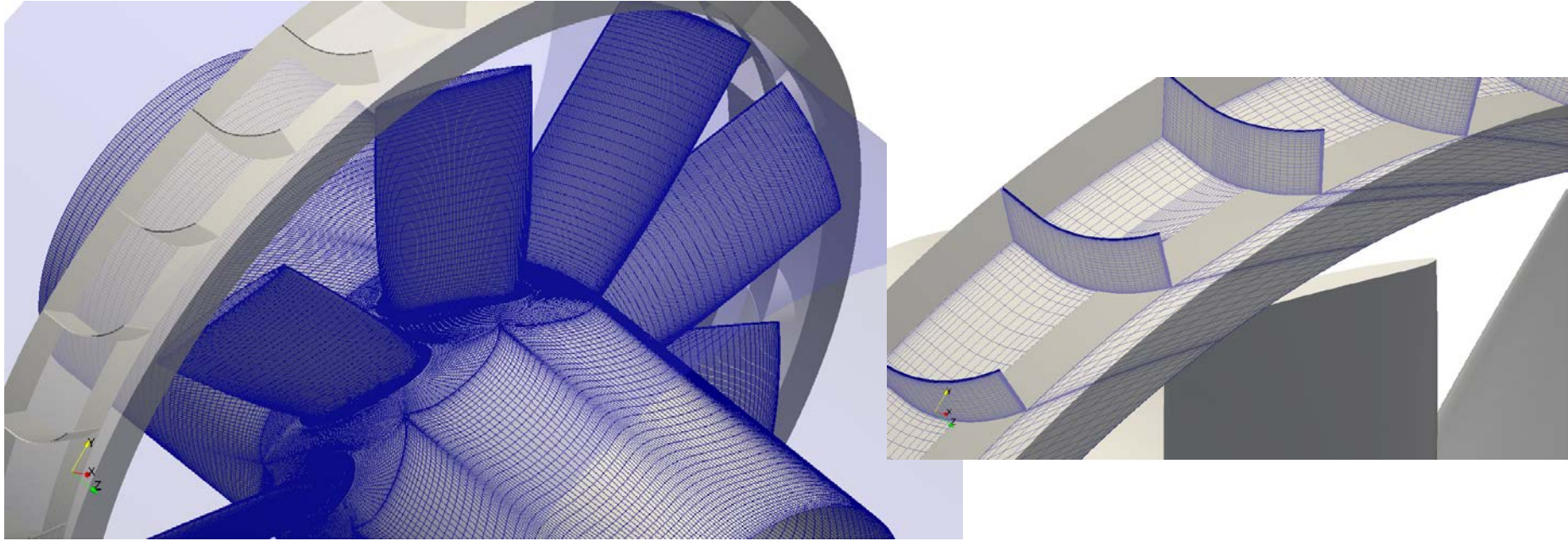


STALL CONTROL MECHANISM

***2. UNSTEADY ROTOR STATOR INTERACTION:
URANS WITH MOVING MESH AND AMI COUPLING***



2. INVESTIGATION OF STALL CONTROL MECHANISM WITH UNSTEADY RANS



Computational domain extend 1 chord upstream of the rotor and 2.5 chords downstream

The final grid was built using 112.5M hexahedra for the fan and 10.8M hexahedra for the stabilization ring – grid independency was tested using total pressure rise and efficiency as convergence parameters

(number of cells = 13.5 times that of the previous grid for steady RANS)

finite volume, opensource, unstructured, parallel, C++

solver: pimpleDyMFoam

U-RANS with cubic k- ε model of Lien and Leschziner

Convective scheme: QUICK

Time integration: 2nd order

Linear solver: conjugate gradient on all quantities with 10^{-7} convergence threshold

CFL

- average 0.02
- maximum: 10

Operating conditions

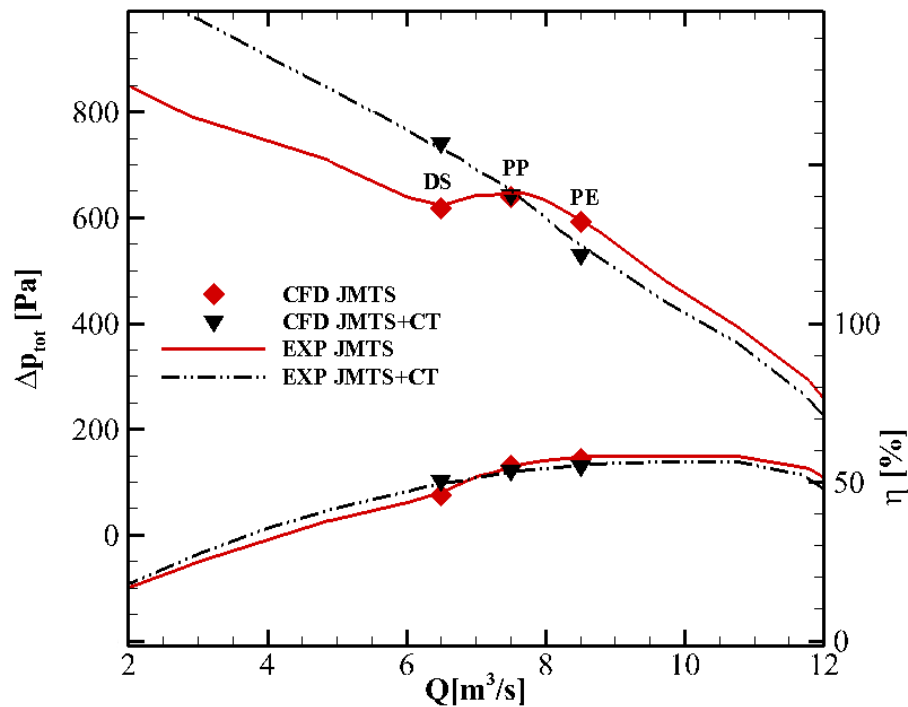
$Q_1 = 8.5 \text{ m}^3/\text{s}$	Peak Efficiency (PE)
$Q_1 = 7.5 \text{ m}^3/\text{s}$	Peak Pressure (PP)
$Q_1 = 6.5 \text{ m}^3/\text{s}$	Deep Stall (DS)

Boundary conditions

<i>Inflow</i>	Mass flow rate TI = 5%; $L_t = 0.07D$
<i>Outflow</i>	Zero gradient
<i>Solid walls</i>	No-slip conditions

2.5 rotor revolutions were simulated

statistics were averaged over 1.8 revolutions

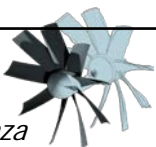


The methodology allowed to reconstruct the curves with fair agreement for all the operating points

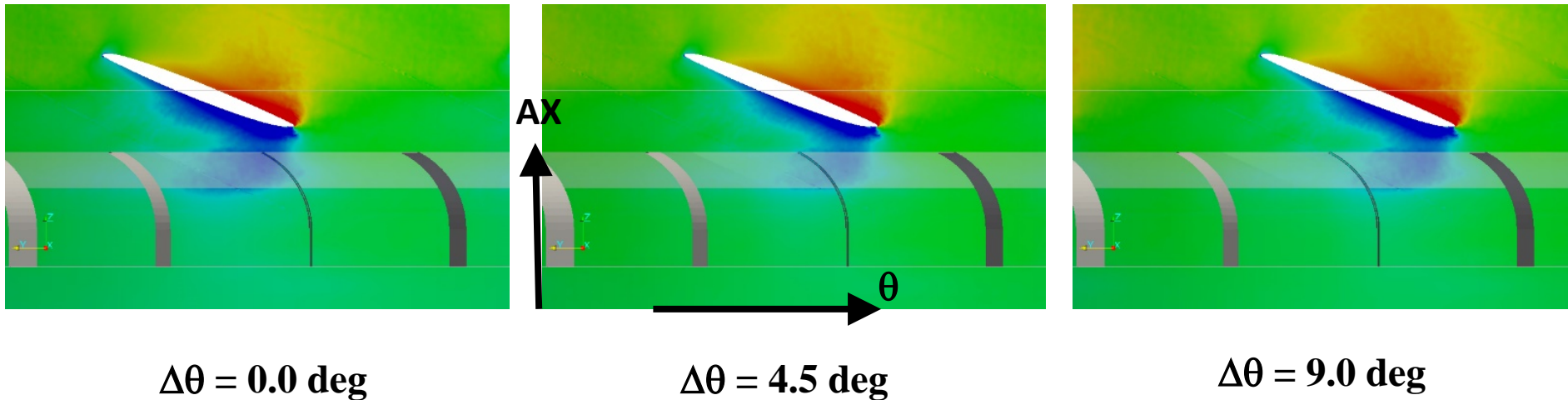
Accuracy of results is within the uncertainty of measurements

Long story short: it still works!

Q [m³/s]		CT	Δp _{tot} [Pa]			η [%]		
		y/n	EXP	CFD	Δ	EXP	CFD	Δ
6.5	DS	y	623	617	0.9%	46.9	45.8	1.1%
		n	730	740	1.3%	49.4	50.2	0.8%
7.5	PP	y	646	639	1.0%	54.6	55.1	0.5%
		n	651	643	1.2%	53.2	53.7	0.5%
8.5	PE	y	595	591	1.0%	57.8	57.2	0.6
		n	548	539	1.6%	55.4	54.9	-0.5



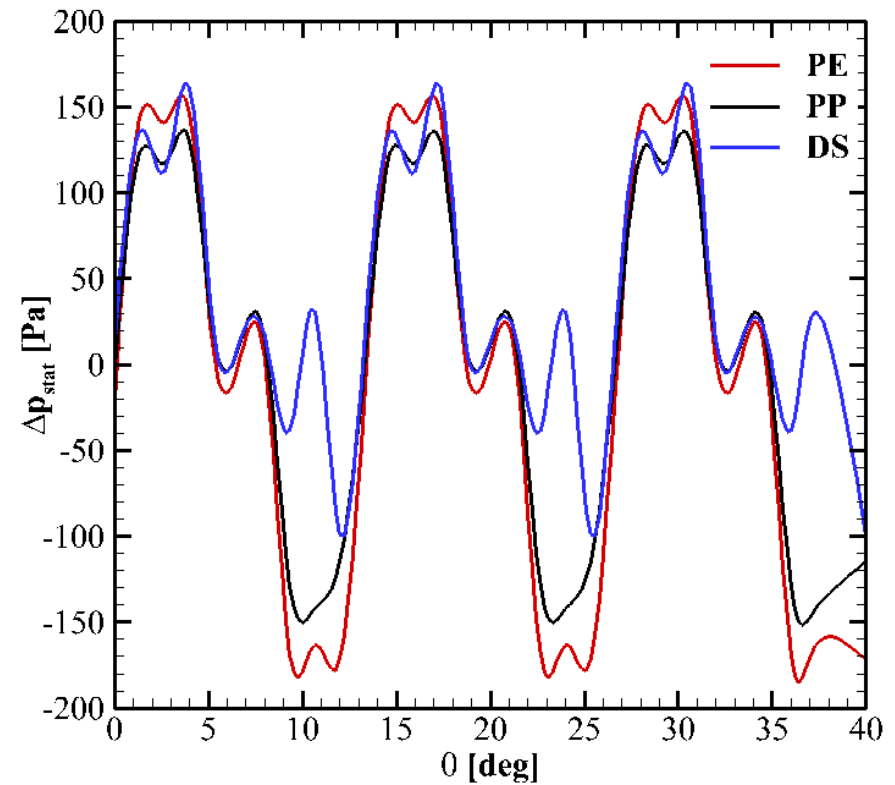
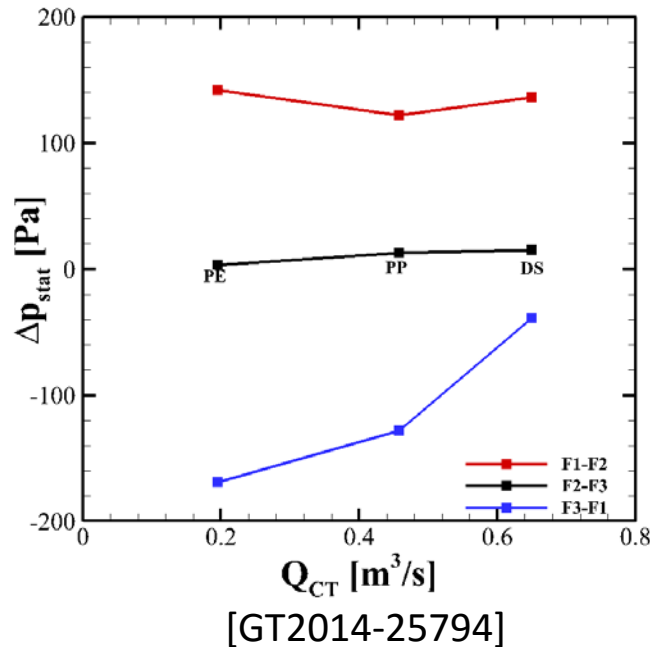
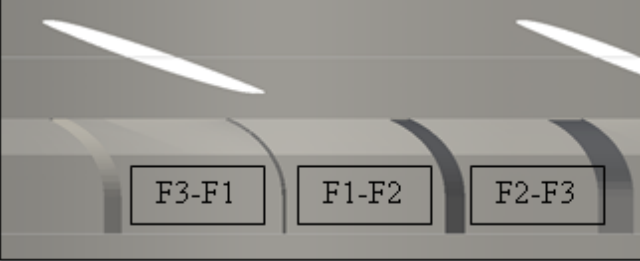
DEEP STALL



In DS operations the low-pressure core contracts when moving from $\Delta\theta = 0$ deg to $\Delta\theta = 4.5$ deg and grows back moving from $\Delta\theta = 4.5$ deg to $\Delta\theta = 9$ deg

Similarly a small increase of the high-pressure core is recognizable moving from $\Delta\theta = 0$ deg to $\Delta\theta = 9$ deg

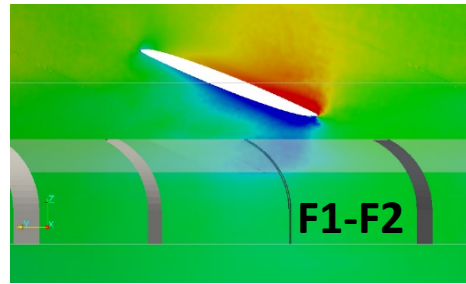
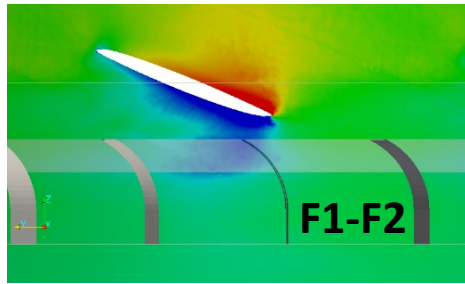
PRESSURE CHARACTERISATION OF THE ANTISTALL RING



40 deg of rotor revolution = the rotor passing three fins of the stabilisation ring

The pressure fluctuations have a frequency that is equal to 1/3 of the BPF so equal to the frequency of the fins.

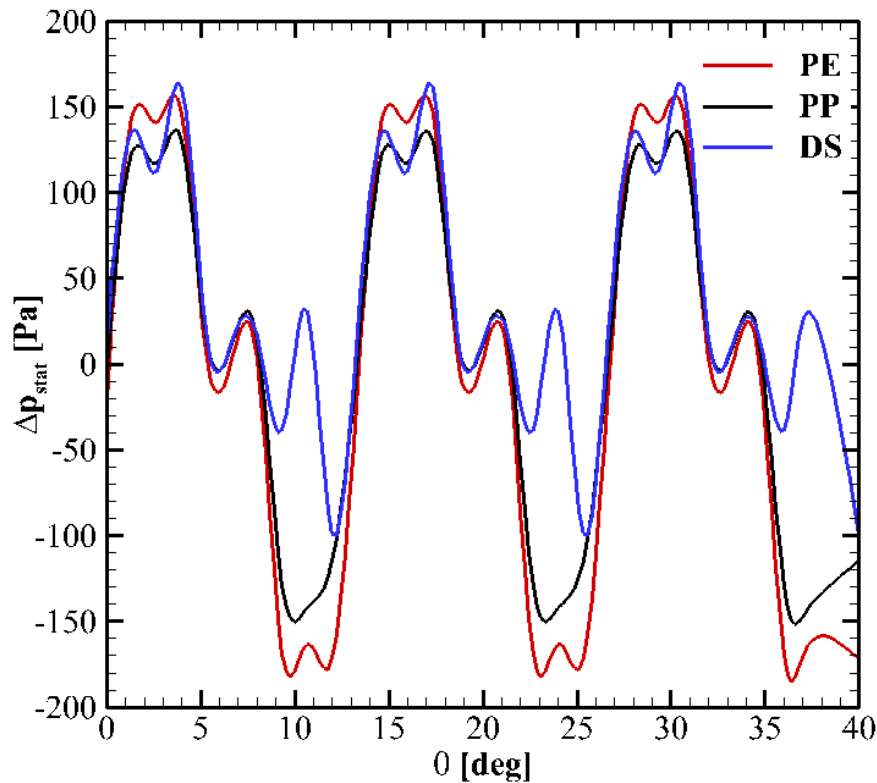
PRESSURE CHARACTERISATION OF THE STABILISATION RING

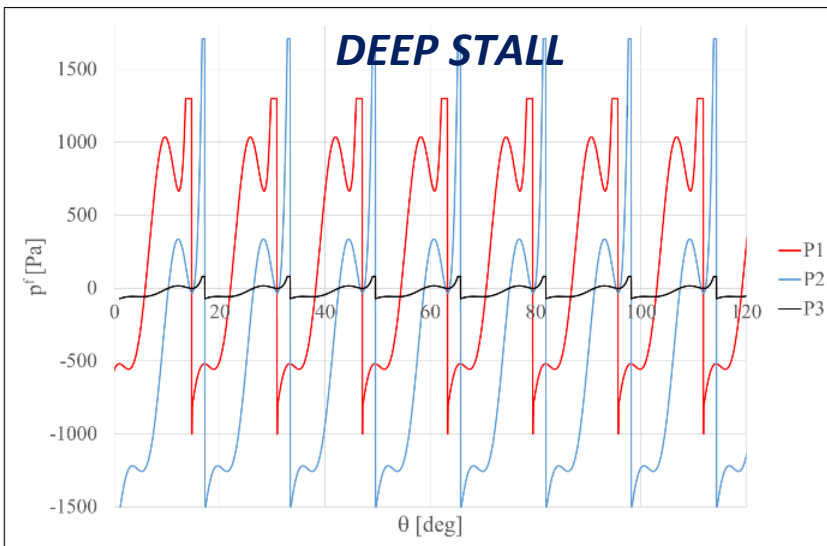
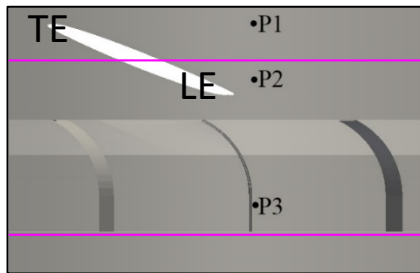


The major difference at DS is in the behaviour in the middle of the signal: at PE and PP the flow was mostly undisturbed and pressure difference dropped.

Here, the low pressure core is much larger and basically a second smaller core appears upstream of the first.

This reflect in the fact that the pressure difference drops, rises again and then drop again (around $\theta = 10$ deg)





The major difference when comparing the three operating points is that the frequency of the fluctuations differs; in particular at DS the frequency is $1/3$ of the BPF that corresponds to the frequency of the fins and the shape of the signal appears as bimodal

At PP the frequency of the oscillations is 2 times the BPF of the rotor with a sinusoidal shape

At PE finally the frequency is $2/3$ of the BPF

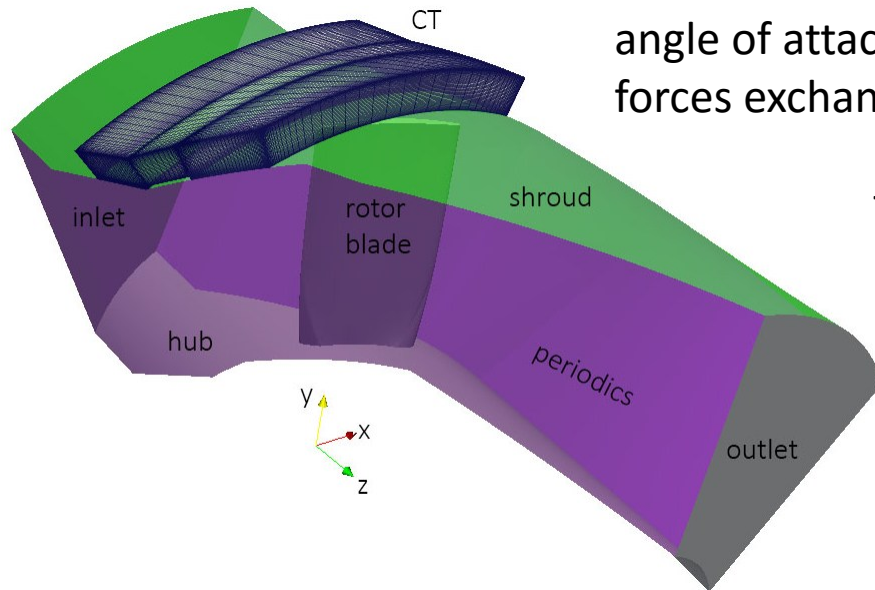
ANTISTALL RING OPTIMIZATION
3. RANS WITH MRF, AMI COUPLING &
ANTISTALL RING MODELLED WITH AN ADVANCED ACTUATOR DISK

3. ANTISTALL RING OPTIMISATION

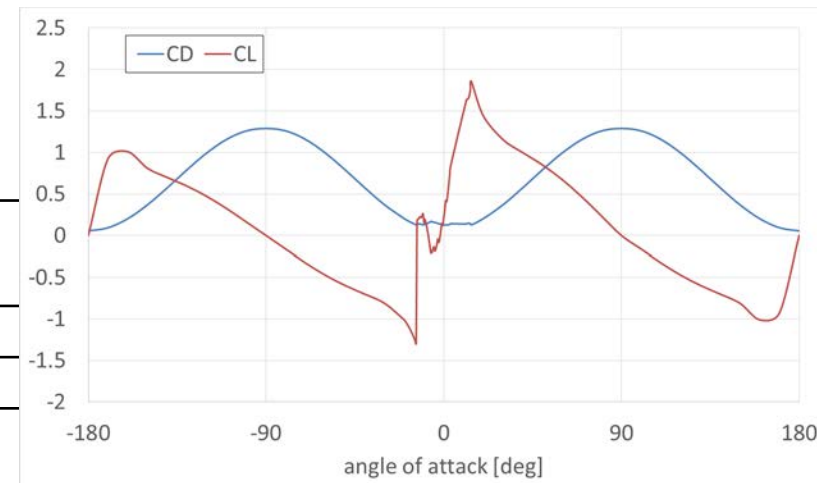
Fins in the antistall ring are not meshed but modelled according to an improved actuator disk technique developed at *Sapienza TITm*

The code computes at runtime for each cell in the actuator disk angle of attack with according to local velocity and computes forces exchanged with the fluid using polar curves given as input

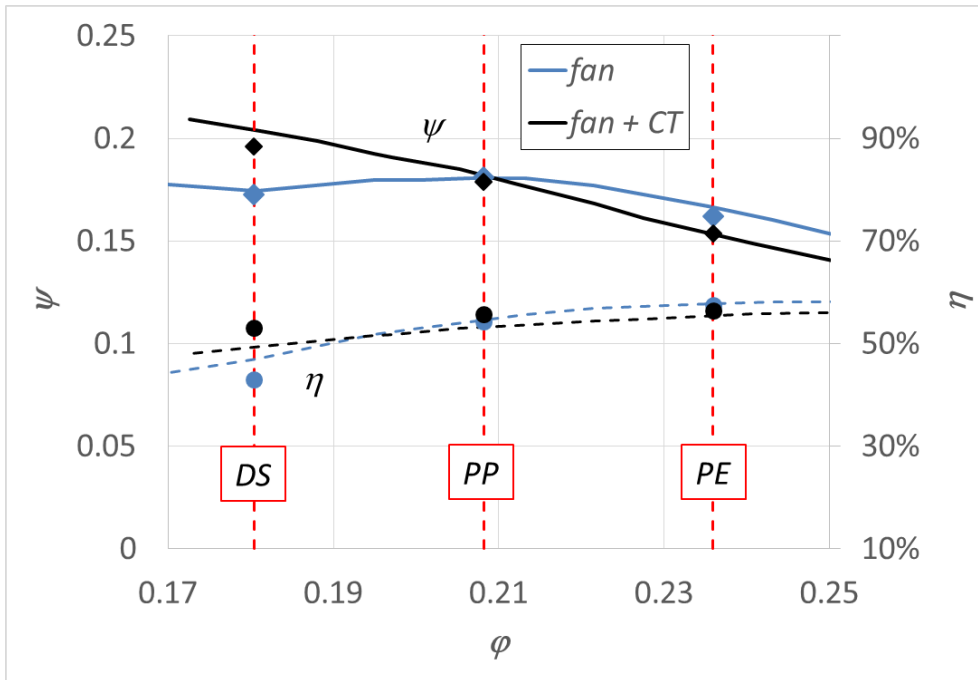
The blade is modelled as a series of sections and linear interpolation of CL and CD between section is assumed



	<i>Number of cells</i>	<i>Error on Δp</i>	<i>Error on Torque</i>
Fine	2,800,000	1.8%	2.1%
(mesh has 30% of the cells used for RANS solution in case 1)			

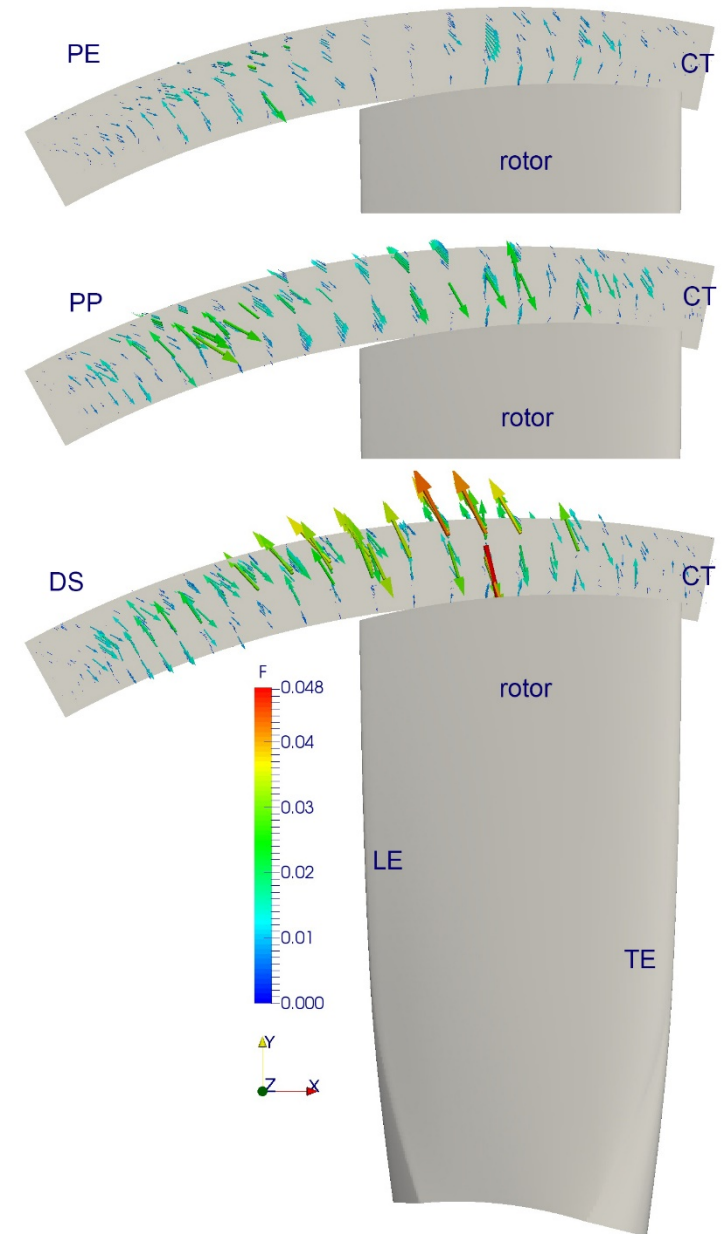


polar curves for antistall ring fins



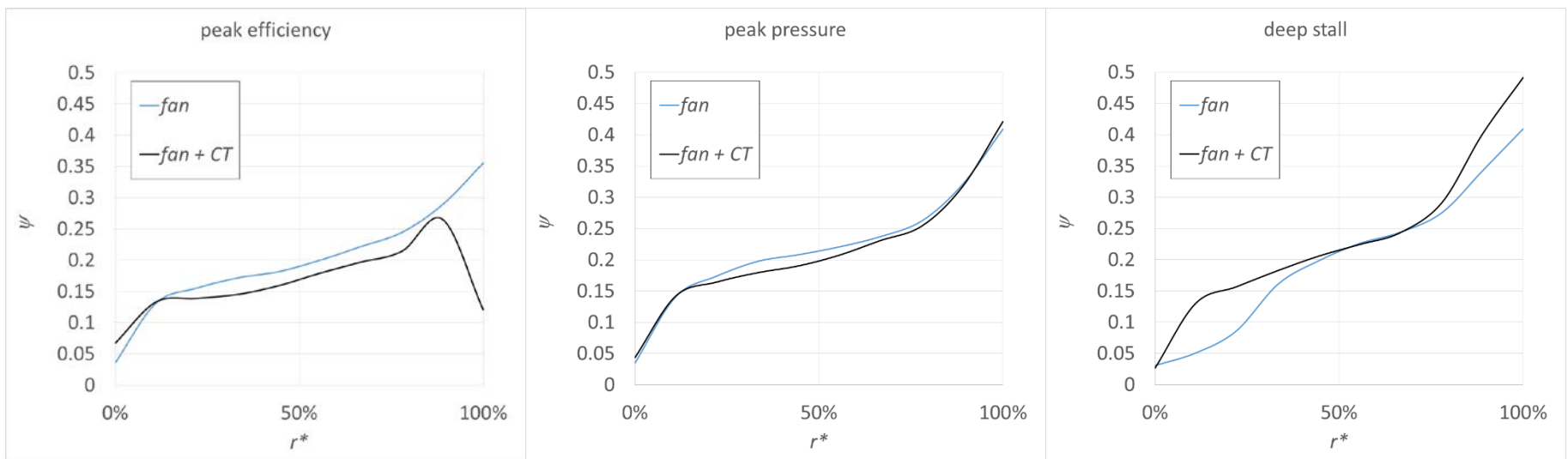
Basically... it still works
(as per previous (1 and 2) cases)

Please notice that here performance curves are
normalised

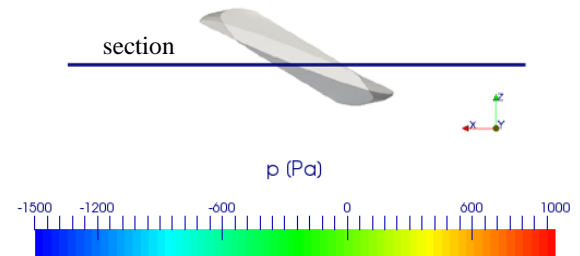


With this approach is easy to change the properties of the fins (shape, pitch angle and so on)
 It is also possible to change the shape of the anti-stall ring (automatic meshing of a simple geometry can be easily done by *snappy*)

We can easily derive characteristic curves of the fan (previous slide) as well as radial distribution of quantity of interest for rotor design

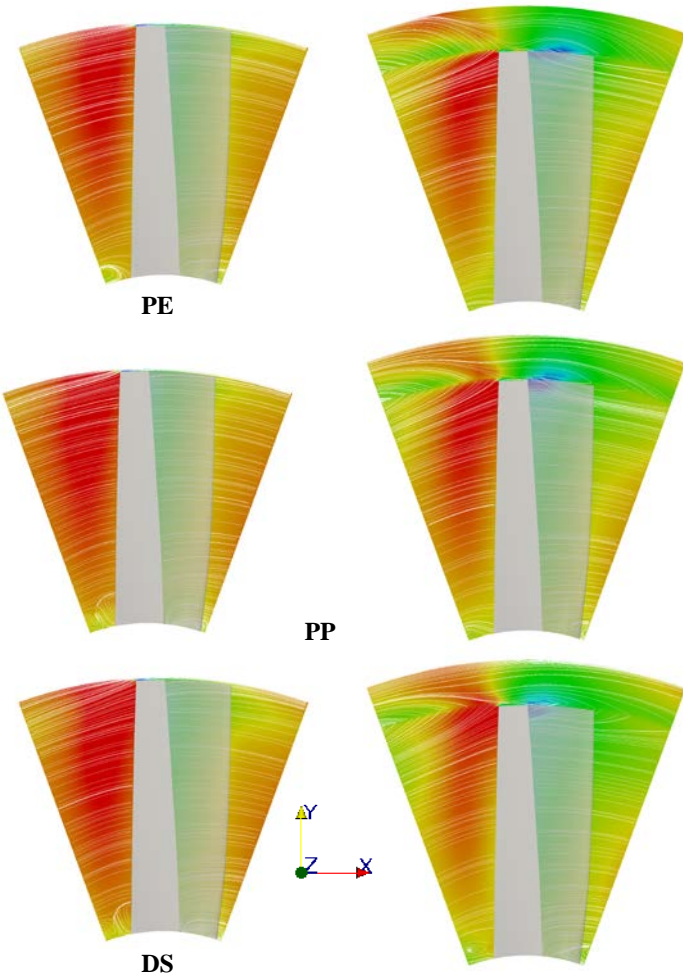


Radial distribution of blade loading coefficient at peak pressure.
 Blue line: baseline fan. Black line: fan with CT.



It is also possible to visually inspect the flow features

Even if not useful in an automatic optimisation loop flow features investigation can unveil unpredicted loss mechanisms to be corrected of features that can be exploited to increase pressure rise and/or efficiency



This work was carried on by me and my colleagues in Rome & Atlanta

Prof. Alessandro Corsini, Dr. Geoff Sheard, Mr. David Volponi and Mr. Tommaso Bonanni

If you want to have a clear understanding of what we did here are [some references](#)

Stall control mechanism investigation:

1. Steady state frozen rotor investigation: RANS with MRF and AMI coupling
Corsini et al. GT2014-25794
2. Unsteady rotor stator interaction: URANS with moving mesh and AMI coupling
Corsini et al. GT2015-42170

Antistall ring optimization

3. Novel strategy to account for the effect of the fins: RANS with MRF, AMI coupling and antistall ring modelled with an advanced actuator disk
Bonanni et al. GT2016-56862(*)

(*) accepted for publication, will be distributed mid-June